Materials Research. 2025; 28:e20240551
DOI: https://doi.org/10.1590/1980-5373-MR-2024-0551

Synthesis and Application of $SnCl_2.H_2O$/ZnO Photoanodes

Vanja Fontenele Nunes[a*], *Francisco Marcone Lima*[b], *João Pedro Santana Mota*[b], *Ana Fabíola Leite Almeida*[b], *Francisco Nivaldo Aguiar Freire*[b], *Antônio Sérgio Bezerra Sombra*[a]

[a] *Universidade Federal do Ceará, Departamento de Física, Fortaleza, CE, Brasil.*
[b] *Universidade Federal do Ceará, Departamento de Engenharia Mecânica, Fortaleza, CE, Brasil.*

Received: December 5, 2024; Revised: March 3, 2025; Accepted: April 2, 2025

Semiconductors films have many applications, energy conversion is one of the main ones. Oxides are often the material used to fabricate these films. Electrophoresis technique can deposit oxides semiconductors at different voltages and time. Films of zinc oxide (ZnO) were electrodeposited on conductive glass, adding weight percentage of tin chloride to improve its photo catalytic properties. The films and cells were characterized by X-ray, UV-Vis and EIS. The characterization showed that higher voltage decreased the band gap value from 3.3 to 3.26 eV, below the average for pure zinc oxide, around 3.30. The films acted as photoanodes in solar cells, with maximum current density of 2.88 mA/cm^2 and open circuit of 0.68 V. The synthesis method was efficient and can be used for further reseach into semiconductors' films and be applied for membranes, photoanodes and other applications.

Keywords: *Electrophoresis, Zinc Oxide, Solar Cells, Films, Synthesis.*

1. Introduction

The electrophoretic method has been applied for thin films on applications such as supercapacitors, biomedical coatings and photovoltaic activity, and deposition of composites[1-4]. It is a simple yet efficient method to deposit thin films, with the electrode (FTO-fluorine tin oxide), the counter electrode (graphite or platinum), and electrolyte (the solution containing the element to be deposited on the FTO). The parameters to be controlled are the voltage and the deposition time of the power source. The interface and the controlling of the parameters is easy and can be done with no additives, no vacuum and at room temperature. The process is more simple than hydrothermal or vacuum deposition, and it does not require heat addition, which can be favorable for the environment and lower costs associated. However, there are some problems associated with the crystalline quality of the films deposited, that can be fixed with the appropriate combination of voltage, time and solution concentration.

Dye sensitized solar cells (DSSC) are third generation solar cells, composed by a photoanode, an electrolyte and a dye, which harvest the absorbed photon that goes through the photoanode and is recovered by the counter electrode and regenerates the electrolyte redox iodide/triiodide[5,6]. The main semiconductor used for photoanode in DSSCs is the titanium dioxide (TiO_2)[7,8], however ZnO has been researched as an viable option due to its properties such as band gap energy (Eg) around 3.30 eV, chemical stability, low costs and non-toxic characteristics[4].

The DSSCs assembled with ZnO still need improvement of its photocurrent efficiency, due to problems in the structure of the cell such as the electron recombination between the ZnO/electrolyte, or ZnO/dye or ZnO/counter electrode interface. Also, the resistances at these interfaces block the electron flow inside the cell, reducing the overall efficiency. Doping or combining the ZnO with elements like tin, titanium, indium, niobium, graphene and many others has been an option to overcome the efficiencies barriers found in the ZnO based DSSC[9-12].

The present study intends to further the research on thin films applied to solar cells, this time using a deposition method, electrophoresis, which is mostly used in biomedical research[13-16]. Other authors use for the synthesis of membranes[17]. The aim is to create good crystalline films with high optical quality and improved conductivity characteristics. Films with those aspects can be applied to optical devices, semiconductors, ultraviolet detectors, solar cells and membrane for batteries.

The authors have done research in the EPD method, and intend with this work to try to improve the use of this synthesis method in the materials engineering field, specific on the renewable energy area, that is crucial and strategic worldwide. The deposition of the films also combines the ZnO with tin chloride, at higher mass percentages, as a way to improve the efficiency of the DSSCs.

2. Methodology

2.1. Deposition of the thin films

The solution of the $SnCl_2.H_2O$/ZnO was done with 8 g/L of ZnO powder (Vitec) and 0.1 g/L of magnesium nitrate (Dinamica); it was added to the zinc oxide solution 15%

*e-mail: vanjafnunes@gmail.com

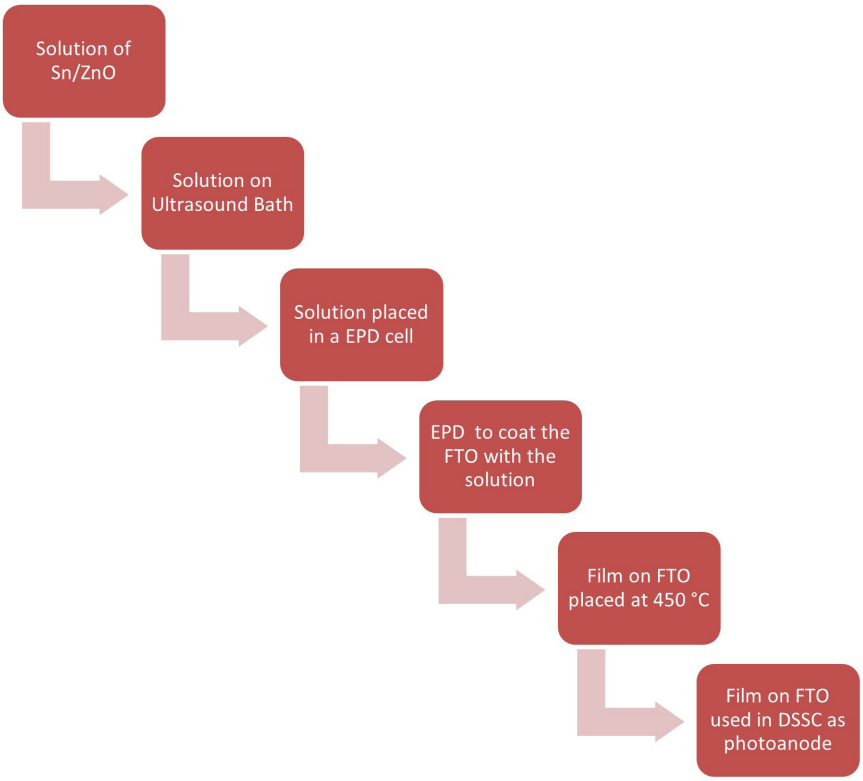

Figure 1. Flowchart with the methodology.

of $SnCl_2.H_2O$ (Dinamica) weight percentage. The solution was to take an ultrasound bath for 15 minutes. The solution was then used as an electrolyte in the electrophoresis cell. The electrode was conductive glass of FTO and the counter electrode was platinum. The deposition for each film lasted 5 minutes, at 30 V, 40 V and 50 V applied by an external ddp source (k33-300V, Kasvi). After 5 minutes, the FTO/Sn/ZnO films were thermally treated at 450°C for 30 minutes. The treatment was done in a muffle furnace F-3000 EDG, with a ceramic heater (220V). Figure 1 has the flowchart explaining the current methodology.

2.2. Assembly of the cell

The Sn/ZnO films after thermal treatment were covered with dye for 24 hours, the dye used was N719 ruthenium based (Solaronix). The film on FTO glass was immersed in the dye for 24 hours before being placed in the sandwiched structure of the cell. The film had active area of 0.25 cm^2. The FTO with the films deposited and covered with dye were then used as electrodes sandwiched with FTO deposited with platinum. Between them, the electrolyte was applied with an injection of AN-50 iodolyte (Solaronix). The scheme of the DSSC cell is represented by Figure 2.

2.3. Characterization

The electrophoresis deposited films were characterized by X-Ray by a Rigaku DMAXB between 20° and 70°; UV-Vis spectrophotometer Shimadzu UV-2600 equipped with ISR-2600Plus; The cell was characterized by an illumination of 100 mW/cm^2, with a white LED, controlled through

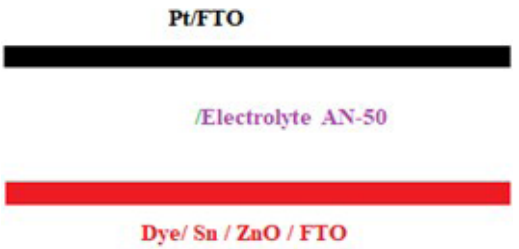

Figure 2. Scheme of the DSSC.

the NOVA1.10 interface program, using an AUTOLAB (PGSTAT302N, Metrohm) that also performed the impedance tests. The tests were performed in room temperature, around 25°C.

3. Results

3.1. X-Ray analysis

Crystallite size according to the Scherrer equation (Equation 1) was 78.3 nm for the 30 V and 15% tin chloride ZnO film.

$$D = \frac{k * \lambda}{\beta * coscos\,\theta} \quad (1)$$

Figure 3 A, B and C has the patterns for the films at 30, 40 and 50 V, respectively. Where D is the crystallite size;

k is equal to 0.9; λ is the wavelength for the Co X-Ray (15.42 nm); β is the FWHM and ɵ is the incident angle (Table 1). The peaks for the ZnO were: (100); (002); (101); (102); (110); (103); (200); (112) and (201) (Figure 3 A). The peaks for the FTO (SnO_2 doped with fluoride) were: (110); (101); (200); (211); (220); (310) and (301). Same observed in[18] with the (002) peak also at 34.3°. The pattern also follows[12,19].

Crystallite size according to the Scherrer equation was 70.6 nm for the 40 V 15% tin chloride. The peaks for the ZnO structure were (100); (002); (101); (102); (110); (103); (112) and (201); and for the FTO (110); (101); (200); (211); (220); (310); (301) (Figure 3 B). Same distribution of patterns in[12] (Table 2).

Figure 3 C has the X-Ray diffraction patterns for the 50 V 15% tin chloride. The peaks of ZnO were (100); (002) and (101) as the main ZnO hexagonal formation at 37.2°; 40.32° and 42.5°, respectively (Table 3). The Scherrer

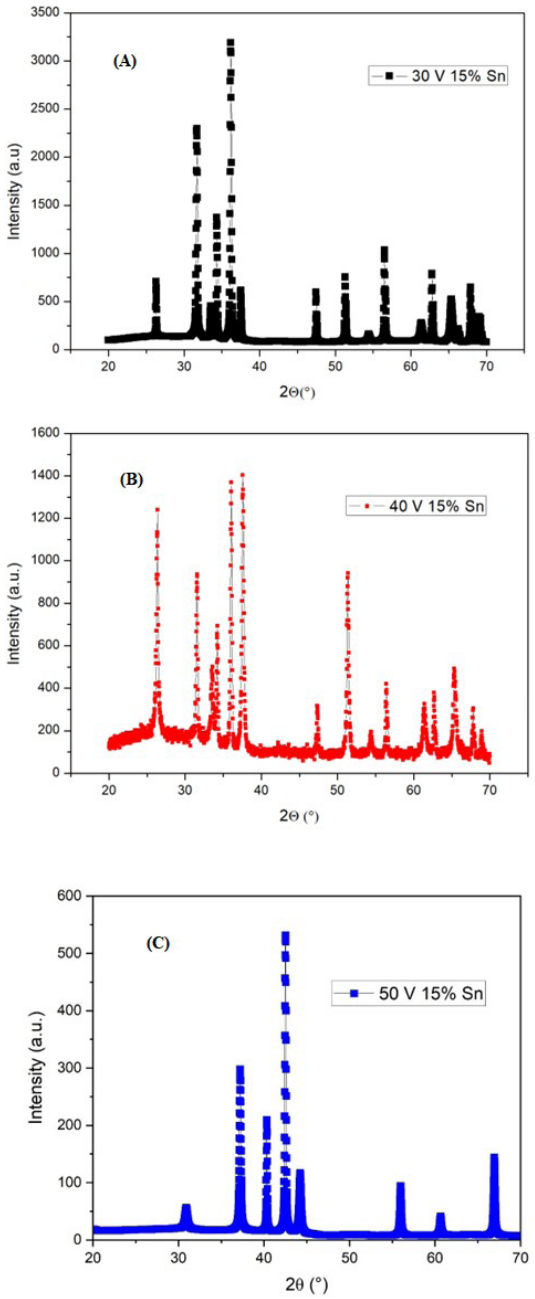

Figure 3. XRD patterns for the three films (A) 30 V (B) 40 V (C) 50 V.

Table 1. Film at 30 V and 15% tin chloride.

Peaks (°)	*(hkl)*
26.4 (FTO)	**(110)**
31.7	(100)
33.8 (FTO)	**(101)**
34.3	(002)
36.2	(101)
37.5 (FTO)	**(200)**
47.5	(102)
51.3 (FTO)	**(211)**
54.4 (FTO)	**(220)**
56.5	(110)
61.4 (FTO)	**(310)**
62.8	(103)
65.3 (FTO)	**(301)**
66.3	(200)
67	(112)
69	(201)

Table 2. Film at 40 V and 15% tin chloride.

Peaks (°)	*(hkl)*
26.4 (FTO)	(110)
31.7	(100)
33.6 (FTO)	(101)
34.4	(002)
36.5	(101)
37.6 (FTO)	(200)
47.4	(102)
51.3 (FTO)	(211)
54.4 (FTO)	(220)
56.4	(110)
61.4 (FTO)	(310)
62.7	(103)
65.3 (FTO)	(301)
67.8	(112)
69	(201)

Table 3. Film at 50 V and 15% tin chloride.

Peaks (°)	*(hkl)*
30.9 (FTO)	(110)
37.2	(100)
40.3	(002)
42.5	(101)
44.15 (FTO)	(200)
55.9	(211)
60.9 (FTO)	(211)
66.9	(110)

equation obtained 40.89 nm. The tin oxide found related to the FTO base was : 30.9° (110); 44.15° (200) and 60.9° (211). The x-ray for the 50 V had less peaks, than the films at 30 and 40 V, there was no formation of different phases such as ZnSnO composites.

It is possible to assume that the higher voltage reduced the size of the peaks and its crystallinity, as obtained by the results of crystallite size and the intensity of the peaks as observed in Figure 3 A, B and C. The crystallinity quality decreases with the higher voltage applied in the electrophoresis method.

It was possible to observe that the film deposited at 40 V had less peaks of FTO than the 30 V and 40 V films, which helped to lower the average crystallite size of the films,

Table 4 shows the cell parameters of the Sn/ZnO films. The change of voltage changes slightly a and b, as also the volume of the cell, that is expected with a voltage increase, and the cell density. The parameters of alpha, beta and gamma were unaltered.

There was a small shrinkage in crystallite size, from 78.3 to 70.6 nm, also observed in[12] when increasing the voltage from 30 to 40 V. Table 2 has the position of the peaks. It can be observed that the increase in voltage decreased the intensity of the peaks from 30 V to 40 V, which can be due to a decrease of the crystallite size. The FTO peaks were also more prominent in the 40 V deposited ZnO film. The reason the x-ray does not show significant change on the ZnO phase is the ionic saturation of the tin in the hexagonal structure. This saturation often changes in relation to the ion, if it is titanium, or tin, or niobium, etc.; and it also changes according to the deposition method, electrophoresis, spin coating, dip coating, hydrothermal, and so forth.

3.2. UV-Vis analysis

The band-gap energy for the films was calculated through the Kubelka-Munk method applied following Equation 2 and 3[20]:

$$F(R)=\frac{K}{S}=\frac{(1-R)^2}{2*R} \quad (2)$$

$$\left(F(R)*hv\right)^2 = A(hv-Eg) \quad (3)$$

Where K is the absorption coefficient; S is the scattering coefficient and R is the reflectance observed in the UV-Vis tests. The band gap energy is estimated by plotting the $(F(R)*hv)^2$ *versus* hν (h is the Planck constant and ν is the photon frequency). A linear fit crossing the x-axis gives the value for the band gap. This value was calculated to be 3.3 eV for the film at 30 V, 3.26 eV for 40 V and 3.23 eV for 50 V (15% tin chloride). This represents the minimum energy of the photon necessary for the electron inside the film to go through the conduction band of the semiconductor. The zinc oxide band gap is close to the titanium dioxide, usually the most common semiconductor used for the DSSCs. The authors[12] also observed Eg between 3.3 and 3.16 eV for ZnO Mg doped films. Thus, the increase from 30 and 40 V did not significantly change the band gap of the films, caused by the saturation effect on ZnO, that is, above a mass percentage, the tin chloride does not substitute the zinc ions in great volume. The electrophoresis deposition of thin films need to be more explored. This is one of the reasons the authors have found an innovative way to deposit semiconductors in a methodology not greatly explored.

The optical properties also reveal that the ZnO films can be used for applications besides solar cells, such as optoelectronic devices that require high reflectance in the visible range of the spectrum, like LEDs and photodetectors.

Figures 4 A-I show the absorbance, $F(R)*(hv)^2$, and reflectance as functions of wavelength, respectively. The electrodeposition showed to be efficient in the synthesis of films that have good reflectance in the visible range (400-700 nm), and peaks of absorbance in the ultraviolet range (below 400 nm). This indicates that these films could be used as UV detectors. All films had reflectance above 80% in the visible spectrum. There were no peaks besides in the region of the band gap, that indicates there was not a creation of sub levels between the unoccupied and occupied electronic levels of the semiconductor.

The lower band gap value indicated a higher density of donor states at the conduction band of the Sn/ZnO film for the 40 V deposition[21]. The band gap values are in accordance with the ones in[18] for ZnO combined with different percentages of Al. The results indicated that at higher voltage, with tin chloride, the band gap energy decreased, which can be a consequence of a lower crystallite size. A lower Eg should favor the photocurrent inside the cell. When the band gap decreases, the electron energy transition from the highest occupied band to the lower uncopied energy band becomes facilitated, therefore, the excited electron can go through the external circuit, increasing the photon injection and current density. Both the absorbance graphs showed that the band transition did not change with the addition of tin chloride,

Table 4. XRD parameters of the ZnO films.

Parameters	30 V	40 V	50 V
a (Å)	3.2490	3.2530	3.2490
b (Å)	3.2490	3.2530	3.2490
c (Å)	5.2070	5.2070	5.2050
Alpha (°)	90	90	90
Beta (°)	90	90	90
Gamma (°)	120	120	120
Volume of the cell	47.60 (10^6 pm^3)	47.72 (10^6 pm^3)	47.58 (10^6 pm^3)
Cell density	5.68 g/cm^3	5.66 g/cm^3	5.66

around 400 nm in the UV spectrum, typical for the ZnO. The reflectance, however, increased from a little below 80% to around 85% with more applied voltage. The reflectance was higher in the visible range of the spectra for all films.

3.3. Impedance analysis

The impedance graphs from both 30 V, 40 V and 50 V resulted very similarly, with a full semicircle for all cases (Figure 5). The smaller diameter for the 40 V deposited film indicated lower resistance, but not so significantly lower to impact a greater difference between solar cells efficiency[2]. The phase angle reaches 50° for both films, with a steeper inclination at 40 V (Figure 6). The peaks in the Bode plots indicate the recombination at the ZnO/electrolyte surface[5].

The recombination is one of the main reasons for the low efficiencies often found in ZnO solar cells. To reduce this phenomenon the authors try to recombine the ZnO with other elements, such as tin, to try to improve the current passage

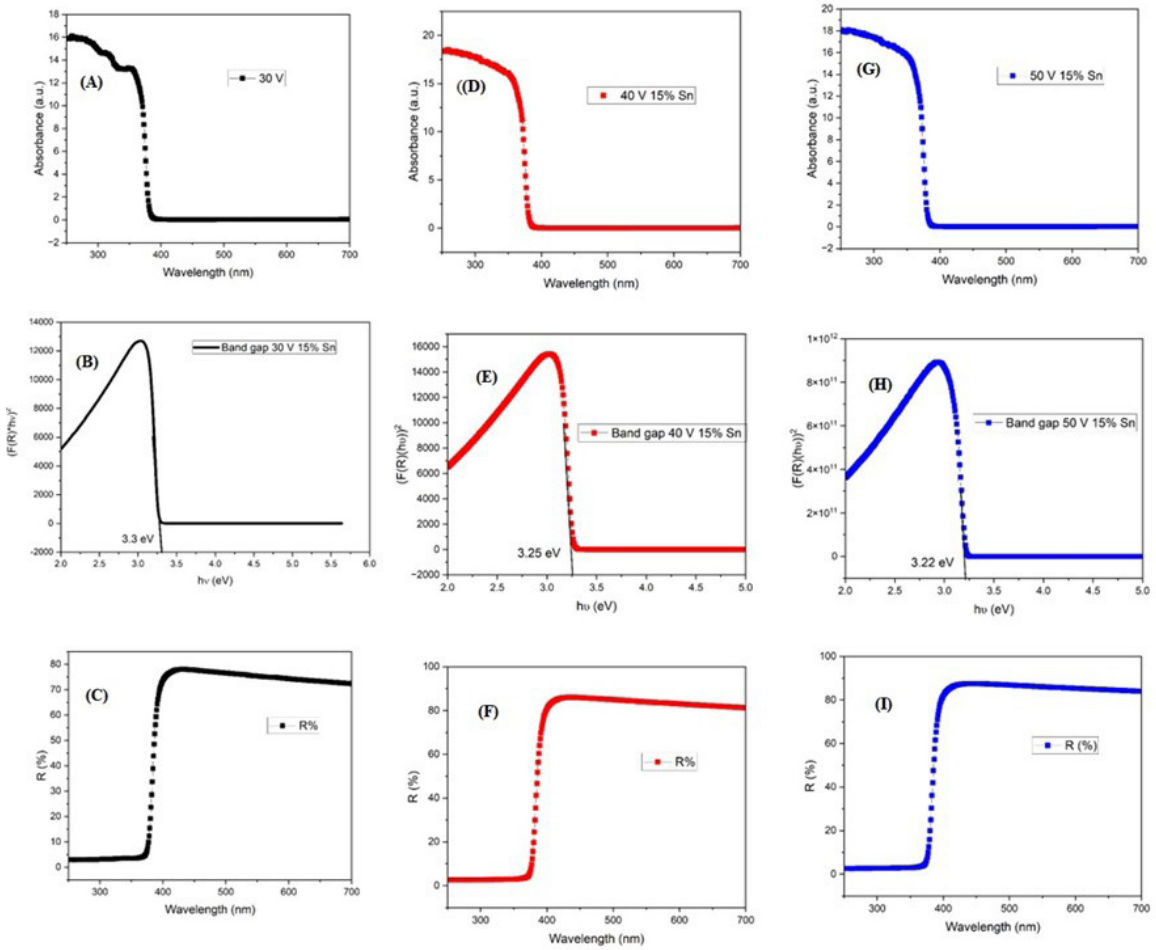

Figure 4. 30 V (A) Absorbance (B) Band Gap (C) Reflectance; 40 V (D) Abs. (E) Eg (F) Reflectance; 50 V (G) Abs. (H) Eg (I) Reflectance.

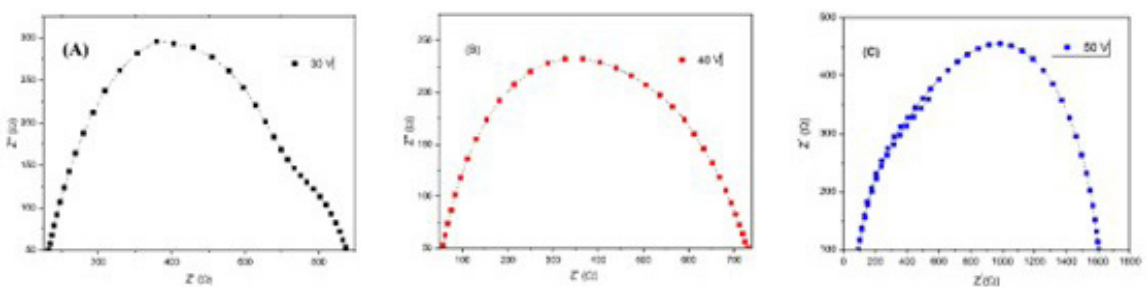

Figure 5. Nyquist plot for the (A) 30 V (B) 40 V (C) 50 V.

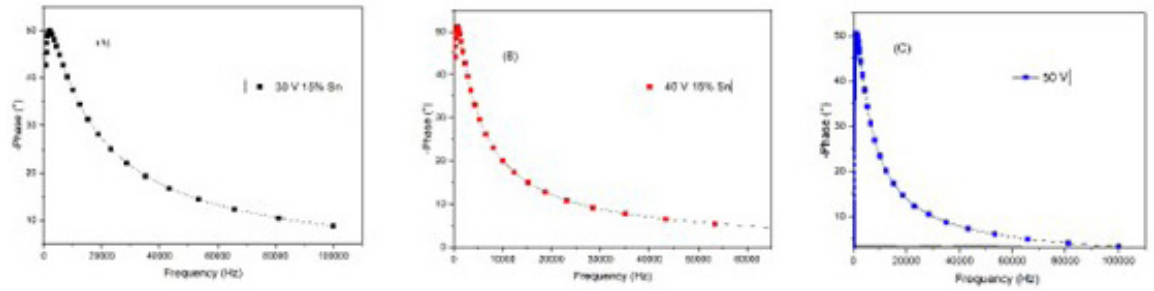

Figure 6. Bode plot for (A) thin film at 30 V (B) 40 V (C) 50 V.

inside the DSSC cell, and reduce the resistance between the interfaces of the cell, ZnO/electrolyte interface; ZnO/dye interface and ZnO/counter electrode interface. Those layers are where most times the recombination occurs

3.4. Photovoltaic tests

The FF (fill factor) was calculated using the Equation 4:

$$FF = \frac{Jmp * Vmp}{Jsc * Voc} \quad (4)$$

Jsc is the short current density and Voc is the open circuit voltage.

When the fill factor is close to 1, the average current and voltage of the cell are in the range as the maximum voltage (Voc) and current (Isc) of the DSSC cell. The Jmp and Vmp are the current and voltage at maximum power (Pmax), respectively. The efficiency was calculated using Equation 5:

$$\eta = \frac{FF * Voc * Jsc}{Pin} \quad (5)$$

Where the Pin, incident power, is 100 mW/cm^2.

The reactions that occur inside the cell are described as in[22]. Equation 6 represents the absorption of the photon by the dye N719, and Equation 7 is the electron transfer through the zinc oxide photoanode.

$$S(dye) + photon \rightarrow S^* \quad (6)$$

$$S^* \rightarrow S^+ + e^- \quad (7)$$

The maximum current density (Jsc) results for both films were similar, 2.8 mA/cm^2, for the 30 and 40 V, however there was a significant decrease for 50 V, with values around 0.37 mA/cm^2 (Figure 7). The lower crystallite size for this film may help to explain this occurrence, since that for 24 hours dye immersion time, the film probably created blockages that increased the resistance to the electric flux through the cell external circuit. The addition of $SnCl_2$ did increase the current density, as noted in[23] the ZnO pure with no added elements is around 1.4 mA/cm^2. However, the fill factor (FF) for the cell at 40 V reduced drastically from 0.43 to 0.26, and picked up again to 0.33 (Table 5), indicating low stability for the cell at

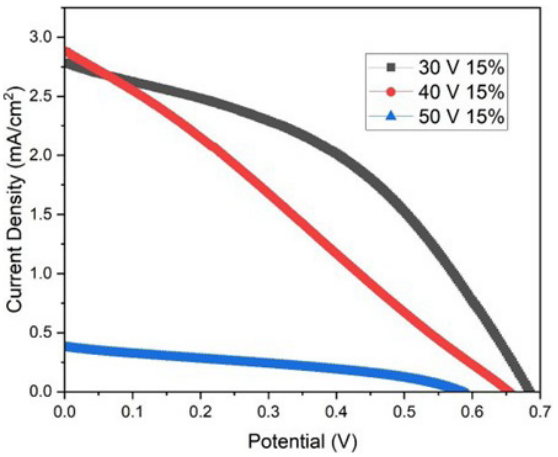

Figure 7. Current density versus potential for the cells.

Table 5. Photovoltaic Parameters for the DSSCs.

Parameters	30 V	40 V	50 V
Voc (V)	0.68	0.66	0.59
Jsc (mA/cm^2)	2.79	2.88	0.37
η (%)	0.82	0.5	0.072
FF	0.43	0.26	0.33

this voltage, which helped to bring down the efficiency for the cell at the voltage parameter. The open circuit voltage (Voc) for both cells was also similar, 0.68 and 0.66 V. These open voltage values are characteristic of the ZnO, and due to the same structure for the cells, FTO/ZnO/Sn/N719/Iodite/FTO, these values tend not to alter significantly.

The lower stability for the 40 V film indicated that the conditions of the 24 hours immersion time in the N719 dye created the agglomerated structures between the ZnO and the ruthenium dye, which is a common cause for lower efficiency in ZnO based DSSCs. Reducing the time of the film in the dye could benefit the overall photocurrent conversion.

The values of efficiency are close to the obtained by[24] using ZnO/PEDOT polymer with efficiencies from 0.49 to 3.29%. Authors in[5] also obtained photocurrent efficiency around 0.85% for TiO_2/GO applied as photoanode in the DSSCs. Additionally[7], had 0.84% efficiency for TiO_2 based dye solar cells. The research in[25] fabricated heterojunction ZnO solar

cells with photocurrent efficiency conversion (PCE) between 0.5 and 0.7%, where for values between 0 and 3% (mol) of aluminum the PCE increased from 0.5 to 0.76, and declined slighted to 0.70 at 6%. This phenomenon is common for ZnO, where, for various elements, the current conversion increases until a certain saturation limit, which changes for every giver dopant element.

Authors in[4] deposited the ZnO films using the same methodology and obtained solar cell efficiency, at 30 V and 5% tin chloride the efficiency was 0.11% and 40 V at 5% was 0.12%. Thus, increasing the tin chloride percentage to 15% increased the overall efficiency, due mainly to the increase in current density from 0.32 and 0.37 mA/cm^2 to2.79 and 2.88 mA/cm^2, at 30 and 40 V (5%) to 30 and 40 V (15%), respectively. Adding more tin chloride helped to increase the current density for the photoanode at 30 and 40 V films, but reduced the efficiency for the 50 V[26], had 2.68% at 50 V with no tin, so it can be deduced that the added of tin reduced the photon injection in the 50 V deposited photoanode[27] obtained efficiency values of 0.16% because the authors were also testing a new combination of rhodamine with TiO_2 in dye solar cells, which is also the intention of this present work, by testing a combination of tin and zinc with EPD.

Those lower efficiency values are affected by the recombination phenomenon, where the electron that should cross over through the semiconductor comes back and reconnects with the electrolyte, instead of being injected into the external layers of the Sn/ZnO electron conductive bands.

4. Conclusion

The electrophoresis (EPD) method deposited efficiently the films of zinc oxide combined with tin chloride at 15% wt. The higher voltage applied reduced the crystallinity quality. The characterization and the application of the films demonstrated that they have potential for photocatalytic application, specifically solar cells. The x-ray synthesized films with higher crystallite size around 80 nm. The maximum current density decreased from around 2.88 to 0.37 mA/cm^2, as indicated by the increase of the internal resistance of the film material, as tested by the Nyquist plots. The absorbance in the UV region indicated that the films can also be applied for UV detectors, and the high reflectance in the visible wavelength can point to the use on transparent devices, such as solar cell in windows. The solar cell activities can be improved by adding another layer of semiconductors such as titanium oxide, or by altering the electrophoresis deposition parameter, such as voltage or time deposition. This paper specifically applied the EPD for solar cell, but the process of the EPD electrochemical cell can be applied for the synthesis of photoanodes used for green hydrogen production.

5. Acknowledgments

The authors would like to acknowledge the CNPq fund number 32/2023 and the CNPq

(Process: 402561/2007-4) Edital MCT/CNPq n◦ 10/2007.

6. References

1. Shaheen I, Hussain I, Zahra T, Memon R, Alothman A, Oulasmane M, et al. Electrophoretic fabrication of ZnO/CuO and ZnO/CuO/rGO heterostructures-based thin films as environmental benign flexible electrode for supercapacitor. Chemosphere. 2023;322:138149.
2. Laybidi F, Bahmari A, Abbasi M, Rajabinezhad M, Beni B, Karampoor M, et al. Electrophoretic deposition of ZnO-Containing bioactive glass coatings on AISI 316L stainless steel for biomedical applications. Coatings. 2023;13:1946.
3. Sung D, Doshi S, Rider A, Thostenson E. Innovative alternating current electrophoretic deposition for micro/nanoscale structure control of composites CS appl. Electron Mater. 2023;5:3715-25.
4. Nunes VF, Maia PHF Jr, Almeida A, Freire F. EPD method for thin films on solar cells. Mater Lett. 2024;358:135896.
5. Sofyan N, Jamil A, Ridhova A, Yuwono A, Dhaneswara D, Fergus J. Graphene oxide doping in tropical almond (*terminalia catappa* L.) fruits extract mediated green synthesis of TiO2 nanoparticles for improved DSSC power conversion efficiency. Heliyon. 2024;10(8):e29370.
6. Visnupriya S, Prabavathi N, Vijayakumar P. Ni-Mo bimetallic oxides/rGO nanocomposites as counter electrode for the application of DSSCs. Chem Phys Impact. 2024;8:100958.
7. Ghani T, Mehmood M, Kanwal H, Naz M, Bashir S. Photovoltaic performance of TiO2 nanotubes anodized under different voltages. Mater Proc. 2024;17(1):24.
8. Venkatraman MR, Rajesh G, Rajkumar S, Ananthan MR, Balaji G. Semi-transparent dye-sensitized solar cells (DSSC) for energy-efficient windows with microwave-prepared TiO2 nanoparticles as photoanodes. Mater Lett. 2024;360:135953.
9. Nunes VF, Almeida A, Freire F. Effects of lithium salt on optical and structural properties of ZnO thin films. Nano Hybrids Compos. 2024;43:57-66.
10. Das A, Das A, Singha C, Bhattacharyya A. Al Mg Co-doped ZnO thin films: effect of the annealing temperature on the resistivity and ultraviolet photoconductivity. Thin Solid Films. 2023;780:139958.
11. Nunes VF, Lima F, Teixeira E, Maia PHF Jr, Almeida A, Freire F. Effects of tin on the performance of ZnO photoanode for DSSC. Materia. 2021;26(4):e13112.
12. Johan B, Ali M, Haque J, Kabir H, Roy S, Ali S. An approach to investigate the structural morphological and optical properties of spray pyrolyzed B and Mg co-doped ZnO thin films. Results Mater. 2023;19:10049.
13. Tan J, Jin S, Huang L, Shao B, Wang Y, Wang Y, et al. A capillary electrophoresis-based assay for carrier screening of the hotspot mutations in the *CYP21A2* gene. Heliyon. 2024;10:e38222.
14. Cheng J, Lv Q, Ji Y, Zhou C, Guo J, Li X, et al. Investigation and elimination of noncovalent artificial aggregates during non-reduced capillary electrophoresis-sodium dodecyl sulfate analysis of a multi-specific antibody. J Pharm Biomed Anal. 2025;225:116673.
15. Maar S, Czuni L, Hassve JK, Takatsy A, Rendeki S, Mintal T, et al. Technical considerations regarding saliva sample collection to achieve comparable protein identification and detection via one- and two-dimensional gel electrophoresis among humans. Heliyon. 2024;10:e40752.
16. Santamária B, Hernandez AL, Laguna MF, Holgado M. Comparative analysis of electrophoresis and interferometric optical detection method for molecular weight determination of proteins. Heliyon. 2024;10:e35932.
17. Lyalin E, Ll'ina E, Kalinina E, Antonov B, Pankatrov A, Pereverzev D. Electrophoretic deposition and characterization of thin-film membranes Li7La3Zr2O12. Membrane. 2023;13(5):468.
18. Ahmir A, Arab L, Meftah A, Latif A. Effect of aluminum doping on the structural optical and electrical properties of ZnO thin films processed under thermal shock conditions. Results Opt. 2023;11:100426.

19. Khalil R, Azar M, Malham I, Turmine M, Vivier V. Electrochemical deposition of ZnO thin films in aprotic ionic liquids: effect of the cationic alkyl-chain-length. J Ion Liq. 2022;2:100031.
20. Makula P, Pacia M, Macyk W. How to correctly determine the band gap energy of modified semiconductor photocatalysts based on UV–Vis spectra. J Phys Chem Lett. 2018;9:6814-17.
21. Widyastuti E, Chiu C, Hsu J, Lee Y. Photocatalytic antimicrobial and photostability studies of TiO2/ZnO thin films. Arab J Chem. 2023;16(8):105010.
22. Bhogaita M, Devaprakasam D. Hybrid photoanode of TiO2-ZnO synthesized by co-precipitation route for dye-sensitized solar cell using phyllanthus reticulatas pigment sensitizer. Sol Energy. 2021;214:517-30.
23. Nunes VF, Lima FM, Teixeira E, Maia PHF Jr, Almeida A, Freire F. Synthesis of TiO2/ZnO photoanodes on FTO conductive glass for photovoltaic applications. Ceramica. 2023;69:79-86.
24. Nadhira A, Mufti N, Aziz M, Sari E, Yuliana E, Abadi M, et al. The brief study of ZnO/PEDOT:PSS counter electrode in DSSC Based on solid electrolyte YSZ. Mater Sci Energy Technol. 2024;7:309-17.
25. Kumar V, Kaphle A, Rathnasekara R, Neupane G, Hari P. Role of Al doping in morphology and interface of Al-doped ZnO/CuO film for device performance of thin film-based heterojunction solar cells. Hybrid Adv. 2024;5:100148.
26. Nunes VF, Teixeira ES, Maia PHF Jr, Almeida AFL, Freire FNA. Study of electrophoretic deposition of ZnO photoanodes on fluorine-doped tin oxide (FTO) glass for dye-sensitized solar cells (DSSCs). Ceramica. 2022;68:120-25.
27. Ranamagar B, Abiye I, Abebe F. Dye-sensitized solar cells on TiO2 photoelectrodes sensitized with rhodamine. Mater Lett. 2023;336:133887.